

Trapping and transporting aerosols with a single optical bottle beam generated by moiré techniques

Peng Zhang,¹ Ze Zhang,^{1,2,3} Jai Prakash,¹ Simon Huang,¹ Daniel Hernandez,¹ Matthew Salazar,¹ Demetrios N. Christodoulides,² and Zhigang Chen^{1,4,*}

¹Department of Physics and Astronomy, San Francisco State University, San Francisco, California 94132, USA

²CREOL/College of Optics, University of Central Florida, Orlando, Florida 32816, USA

³National Key Laboratory of Tunable Laser Technology, Harbin Institute of Technology, Harbin 150080, China

⁴The Key Laboratory of Weak-Light Nonlinear Photonics and Technological Economy Development Area (TEDA) Applied Physics School, Nankai University, Tianjin 300457, China

*Corresponding author: zhigang@sfsu.edu

Received January 28, 2011; revised March 13, 2011; accepted March 19, 2011;

posted March 21, 2011 (Doc. ID 141874); published April 15, 2011

We demonstrate optical trapping and manipulation of aerosols with an optical bottle beam generated by the moiré techniques. We observe stable trapping and back-and-forth transportation of a variety of absorbing carbon particles suspended in air, ranging from clusters of nanosized buckminsterfullerene C₆₀ to micrometer-sized carbon powders. © 2011 Optical Society of America

OCIS codes: 350.4855, 260.6042, 050.0050, 160.4236.

Optical bottle beams are beams with low or null intensity channels surrounded by three-dimensional (3D) regions of higher intensity. Over the past years, a variety of techniques have been proposed for generating such beams for applications in optical tweezers and atom traps [1–7]. Recently, optical bottle beams were established using two counterpropagating vortices in order to trap and manipulate light-absorbing particles in air [8]. In these latter experiments, the photophoretic force was found to dominate [9,10] over gradient forces that are typically exerted on transparent particles in optical tweezing arrangements [11–13].

In this Letter, we design and generate bottle beams from a Gaussian beam by employing the moiré techniques [14]. Assisted with a spatial light modulator (SLM), this class of bottle beams is created and used for demonstration of stable optical trapping and back-and-forth transportation of aerosols. The aerosols consist of different absorbing carbon particles suspended in air, ranging from clusters of nanosized buckminsterfullerene C₆₀ to micrometer-sized carbon powders. While the diameter and length of an optical bottle can be controlled at will, our trapping technique does not rely on phase-sensitive interference or mechanical movement. Simply by translating a focusing lens, the trapped aerosols can be made to oscillate in air. This scheme might be of use in manipulating microparticles and nanoparticles for both atmospheric and biological applications.

The principle for generating an optical bottle beam is illustrated in Fig. 1. Here two different fork gratings obtained by interfering a plane wave with a focusing and a defocusing vortex beam are overlapped to produce the desired moiré pattern [Figs. 1(a)–1(d)]. The topological charge of the vortex illustrated is $m = 3$, but other charges can also be used for different bottle configurations. Similar to the procedure described in [14], the moiré pattern as shown in Fig. 1(d) can be retrieved by optical spatial filtering. Interestingly, such a moiré pattern leads to an optical 3D bottle structure, as a Gaussian beam

passing through the gratings results in a doughnut-shaped beam profile that varies along the propagation direction after proper imaging. A typical example of a simulated optical bottle beam is shown in Figs. 1(e)–1(i), where Fig. 1(e) depicts a side view of this beam propagating along the longitudinal z direction, and Figs. 1(f)–1(i) show snapshots of the transverse intensity patterns at the marked positions in Fig. 1(e). Clearly, the bottle is formed with its two “necks” positioned at planes 2 and 4.

To generate the bottle beam illustrated in Fig. 1, we used the experimental setup sketched in Fig. 2. Note that, in our experiment, the overlapping of two different gratings is done through a computer-controlled SLM [14]

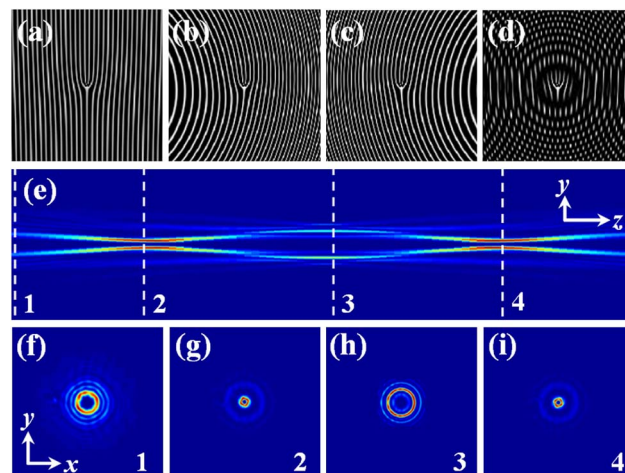


Fig. 1. (Color online) Numerical simulation of optical bottle beam generated with moiré technique. (a) Typical fork grating for a triply charged vortex; (b), (c) single gratings corresponding to (a) but with a focusing and defocusing vortex, respectively; (d) moiré pattern generated by overlapping the two gratings shown in (b) and (c); (e) side view of bottle-beam propagation numerically retrieved from the moiré pattern (d); (f)–(i) snapshots of transverse intensity patterns of the bottle beam at planes 1–4 marked in (e).

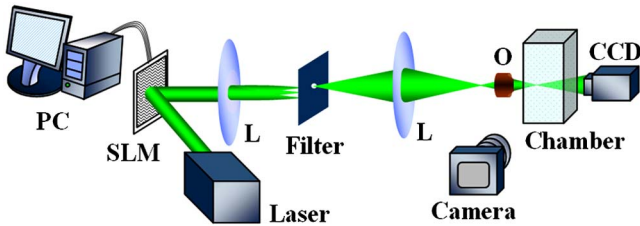


Fig. 2. (Color online) Schematic of experimental setup for generation of optical bottle beam with moiré technique. SLM, spatial light modulator; L, lens; O, objective lens.

without involving any phase-sensitive interferometry or multibeam superposition. The moiré pattern is retrieved by sending a single laser beam into the SLM. Upon reflection from the SLM, the beam is properly filtered and focused into a glass cuvette that is used as a gas chamber. The side view of the beam is captured by a high-resolution camera, with another CCD camera recording the transverse beam intensity patterns at different propagation distances. The experimental results are shown in Figs. 3(a)–3(e), where Fig. 3(a) provides a direct side view of the bottle beam corresponding to Fig. 1(e). With the triply charged ($m = 3$) vortex hologram programmed to the SLM, the resultant bottle has a beam waist of about $80\ \mu\text{m}$ at the two neck positions (separated by $2.5\ \text{cm}$), and a beam waist of about $180\ \mu\text{m}$ at the central position (maximum waist of the bottle). Yet the bottle structure is clearly visible even from the side-view picture taken from scattered light. Snapshots of transverse intensity patterns of the bottle beam are displayed in Figs. 3(b)–3(e), taken at different longitudinal positions. Clearly, our experimental observation agrees well with our numerical simulation. The apparent double necks arise from the retrieved moiré pattern, which turns the Gaussian beam into two collinear vortices having different wavefront curvatures. So in essence, our bottle generation is similar to the dual-vortex-beam scheme [8], but we only need one Gaussian beam. Single-beam bottle generation was reported before with a different scheme [15]. Here the parameters of the optical bottle beam can be easily controlled by the SLM in real time. For example, the size and intensity of the beam can be varied by changing the topological charge and/or the curvatures of the vortex-beam wavefront through the SLM, along with fine tuning of the lens system.

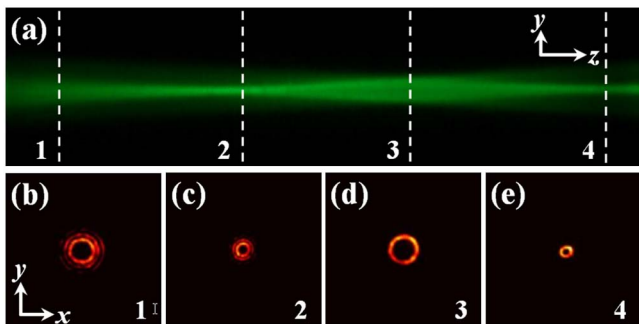


Fig. 3. (Color online) (a) Side-view experimental photography of a single-beam optical bottle, where the two bottle necks are located near planes 2 and 4. (b)–(e) Snapshots of transverse intensity patterns of the bottle beam (contrast enhanced) taken at planes 1–4 marked in (a).

To demonstrate optical trapping of absorbing particles using the above bottle beam, different kinds of carbon aerosols were used. For qualitative observation, we simply employed toner particles from a printer cartridge and spread them in the air near the bottle beam. The toner particles contain carbon powders melted with polymers, and they are aspherical in shape with sizes ranging from 8 to $16\ \mu\text{m}$. Without any camera or imaging system, trapping of these particles was clearly observed, although susceptible to ambient perturbations. To achieve and monitor the stable trapping of aerosols, we launched a much smaller bottle beam (about $20\ \mu\text{m}$ at maximum waist) generated with a single-charged ($m = 1$) vortex hologram into the glass chamber as shown in Fig. 2. Inside the chamber, three kinds of carbon aerosols were tested. The first consists of buckminsterfullerene (C_{60}) nanoparticles, which are smaller (less than a few nanometers) but much denser (density about $1.65\ \text{g}/\text{cm}^3$) than the carbon nanofoam used in a previous experiment [10]. The other two are carbon-based particles purchased from Sigma-Aldrich: carbon nanopowder (particle size $<50\ \text{nm}$) and carbon glassy spherical powder (particle size range is $2\text{--}12\ \mu\text{m}$). All three types of carbon particles were stably trapped in our bottle beam.

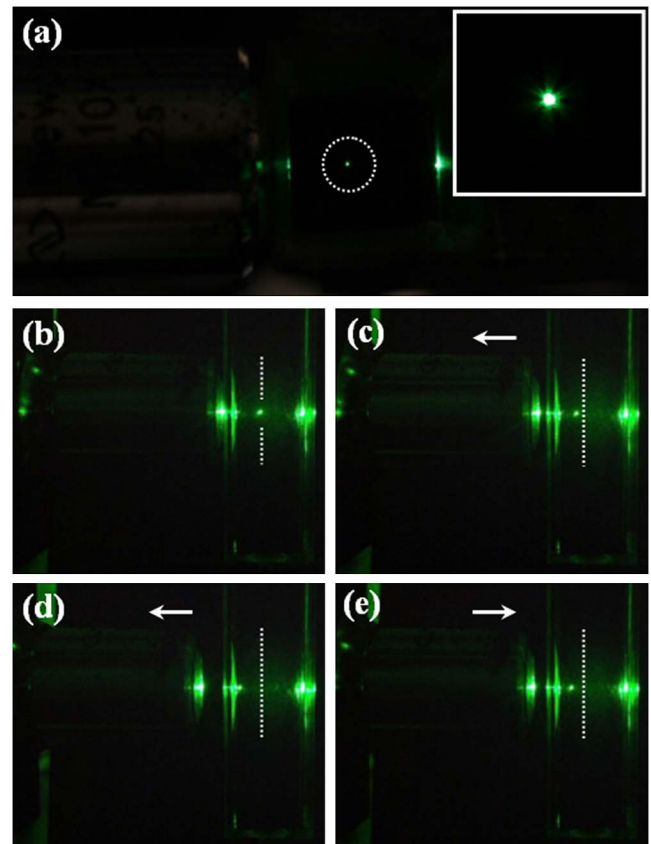


Fig. 4. (Color online) Experimental demonstration of stable trapping of absorbing carbon particles in air. (a) Photograph of trapped particles (bright spot inside dashed circle) as light scatters from the trapped carbon nanoparticles, where inset is the zoomed-in view of the trapped particles; (b)–(e) snapshots from a video taken when the trapped aerosols are transported back and forth inside a glass cuvette by the bottle beam; see Media 1. Dashed line serves as a reference while the arrow shows the movement of focusing (objective) lens.

In Fig. 4 we show a typical example of stable trapping of carbon glassy powder achieved in our experiment. The trapped particles are clearly visible due to scattered light, as seen from the side-view photographs in Fig. 4. The particles are stably trapped so they remain in the trap even in the presence of ambient air vibrations. In fact, they can be moved back and forth by translating the microscope objective lens used for focusing the bottle beam. Such dynamical trapping can be seen clearly in the snapshots of Figs. 4(b)–4(e) and Media 1. Not only can the aerosols be transported readily to a large distance (1 cm path length was used in our experiment but certainly not limited to this distance), but the trap can be “turned” on and off simply by reconfiguring the gratings through the SLM. In fact, our experiments show that, by adaptively changing or reconfiguring the gratings in the SLM, one can reshape or relocate the bottle beam for trapping and manipulation of a large range of absorbing particles.

Given the size of our bottle beam used for the trapping experiment of Fig. 4 (about $20\ \mu\text{m}$ in waist), we believe that, for nanosized particles, a cluster of many such particles are trapped, while for micrometer-sized carbon glassy spherical powders there are only a few particles that stay in the bottle beam. Of course, stable trapping of a single particle is expected if we can make the bottles small enough and comparable to the particle size. Such “microbottles” were established recently with the volume speckle field [16]. For our setting, more controllable experiments are currently underway for measuring the number of particles and monitoring the particle velocity after the trap is turned off. Moreover, with the SLM-assisted beam design, we can expect to develop a dynamical array of bottle-beam traps for 3D trapping and manipulation.

In summary, we have shown that optical bottle beams can be generated and controlled by employing the moiré techniques. With such optical bottle beams, we have demonstrated optical trapping and manipulation of absorbing particles in air. Our results bring about new possibilities for trapping aerosols based on optical bottle

beams in a controllable fashion, which may find applications in optical, biological, and atmospheric sciences.

This work was supported by the National Science Foundation (NSF), the United States Air Force Office of Scientific Research (USAFOSR), and the 973 Program. We thank A. S. Desyatnikov for discussions and A. S. Ichimura and W. Man for assistance.

References

1. J. Arlt and M. Padgett, *Opt. Lett.* **25**, 191 (2000).
2. B. Ahluwalia, X. Yuan, and S. Tao, *Opt. Express* **12**, 5172 (2004).
3. P. Rudy, R. Ejnisman, A. Rahman, S. Lee, and N. P. Bigelow, *Opt. Express* **8**, 159 (2001).
4. D. Yelin, B. E. Bouma, and G. J. Tearney, *Opt. Lett.* **29**, 661 (2004).
5. J. X. Pu, X. Y. Liu, and S. Nemoto, *Opt. Commun.* **252**, 7 (2005).
6. L. Isenhower, W. Williams, A. Dally, and M. Saffman, *Opt. Lett.* **34**, 1159 (2009).
7. P. Xu, X. He, J. Wang, and M. Zhan, *Opt. Lett.* **35**, 2164 (2010).
8. V. G. Shvedov, A. S. Desyatnikov, A. V. Rode, W. Krolikowski, and Y. S. Kivshar, *Opt. Express* **17**, 5743 (2009).
9. A. S. Desyatnikov, V. G. Shvedov, A. V. Rode, W. Krolikowski, and Y. S. Kivshar, *Opt. Express* **17**, 8201 (2009).
10. V. G. Shvedov, A. V. Rode, Y. V. Izdebskaya, A. S. Desyatnikov, W. Krolikowski, and Y. S. Kivshar, *Phys. Rev. Lett.* **105**, 118103 (2010).
11. A. Ashkin, *Phys. Rev. Lett.* **24**, 156 (1970).
12. K. Dholakia, P. Reece, and M. Gu, *Chem. Soc. Rev.* **37**, 42 (2008).
13. D. McGloin and J. P. Reid, *Opt. Photonics News* **21** (3), 20 (2010).
14. P. Zhang, S. Huang, Y. Hu, D. Hernandez, and Z. Chen, *Opt. Lett.* **35**, 3129 (2010).
15. V. G. Shvedov, Y. V. Izdebskaya, A. V. Rode, A. S. Desyatnikov, W. Krolikowski, and Y. S. Kivshar, *Opt. Express* **16**, 20902 (2008).
16. V. G. Shvedov, A. V. Rode, Y. V. Izdebskaya, A. S. Desyatnikov, W. Krolikowski, and Y. S. Kivshar, *Opt. Express* **18**, 3137 (2010).